Non-Hermitian sensing from the perspective of postselected measurements

Neng Zeng ¹ Tao Liu, ¹ Keyu Xia, ^{2,3} Yu-Ran Zhang ¹, and Franco Nori ^{4,5}

¹School of Physics and Optoelectronics, South China University of Technology, Guangzhou 510640, China

²College of Engineering and Applied Sciences, National Laboratory of Solid State Microstructures,

Nanjing University, Nanjing 210023, China

³Shishan Laboratory, Suzhou Campus of Nanjing University, Suzhou 215000, China

⁴Center for Quantum Computing, RIKEN, Wakoshi, Saitama 351-0198, Japan

⁵Physics Department, University of Michigan, Ann Arbor, Michigan 48109-1040, USA

(Received 12 May 2025; accepted 31 October 2025; published 24 November 2025)

By employing the Naimark dilation, we establish a fundamental connection between non-Hermitian quantum sensing and postselected measurements. The sensitivity of non-Hermitian quantum sensors is determined by the effective quantum Fisher information (QFI), which incorporates the success probability of postselection. We demonstrate that non-Hermitian sensors, regardless of the specific form of decoherence or the choice of probe states, cannot outperform their Hermitian counterpart when all information is harnessed, since the total QFI for the extended system constrains the effective QFI of the non-Hermitian subsystem. Moreover, we quantify the efficiency of non-Hermitian sensors with the ratio of the effective QFI to the total QFI, which can be optimized within the framework of postselected measurements with minimal experimental trials. In addition, the performances of non-Hermitian sensors versus different types of technical noises can be judged using our framework. Our work provides a distinctive theoretical framework for investigating non-Hermitian quantum sensing and designing noise-resilient quantum metrological protocols.

DOI: 10.1103/g3n3-gh49

I. INTRODUCTION

Quantum metrology leverages quantum coherence and entanglement to enhance sensitivity and accuracy in measuring physical quantities [1–3], with promising applications in various fields of modern science and technology [4–6]. The achievements of modern quantum physics have also introduced frameworks and protocols for quantum-enhanced metrology [7–12]. Recently, several metrological schemes based on non-Hermitian physics have been theoretically proposed and experimentally demonstrated, e.g., enhanced sensing near exceptional points (EPs) [13–25]. Due to the divergence of the susceptibility in the vicinity of EPs, EP-based sensors have been theoretically predicted to realize enhanced sensing [20]. The EP-based sensors can be realized in \mathcal{PT} symmetric systems with two EPs at the phase transition points of PT-symmetry breaking, which have been demonstrated in open systems with loss and gain [26-29]. Several experiments have implemented EP-based sensing with an enhanced signal-to-noise ratio (SNR) [30–33]. However, some works doubt whether EP-based sensors can improve the fundamental sensitivity limits in the presence of noise [34–38]. In

Published by the American Physical Society under the terms of the Creative Commons Attribution 4.0 International license. Further distribution of this work must maintain attribution to the author(s) and the published article's title, journal citation, and DOI.

addition, another non-Hermitian sensing scheme independent of EPs has been proposed, which is predicted to be robust against some specific forms of noise [39,40]. Whether non-Hermitian sensors can offer an advantage in estimation sensitivity over conventional Hermitian sensors is still a controversial topic [41], despite studies on the metrological limits of non-Hermitian sensing [42–44].

Non-Hermitian sensing involves projection-value measurements (PVMs) merely on the quantum subsystem that exchanges energy with its environment. The quantum open system dynamics are more rigorously described with approaches, such as the Kraus representation and Lindblad formalism [45-47]. For noisy quantum parameter estimation (QPE), the minimum achievable statistical uncertainty is determined by the quantum Fisher information (QFI) and the Cramér-Rao bound (CRB) [48,49]. It relates to the minimal QFI corresponding to a unitary evolution of the enlarged system [50,51]. Thus, from the perspective of quantum information science [52], the metrological resources from both the open system and its environment should be considered when comparing the performances of non-Hermitian sensors and their Hermitian counterparts [44]. This problem is in analogous with the measurement sensitivity of weakvalue-amplification (WVA) technique [53–57], which greatly improves the SNR by discarding most detection trials. WVA can be described as POVMs on the sensor subsystem, interacting with an ancillary system. With the Naimark extension theorem and its inference [58,59], a non-Hermitian system can be dilated to a larger Hermitian system followed by postselecting the ancilla state [60-63]. Therefore, non-Hermitian

^{*}Contact author: yuranzhang@scut.edu.cn

sensing can be understood in the framework of the QPE with postselected measurements, of which the measurement sensitivity in the presence of technical noise has been widely discussed [64–79].

Here, we investigate the sensitivity of non-Hermitian sensors by establishing a fundamental connection between non-Hermitian sensing and QPE with postselected measurements. Analogous to WVA, we show the enhancement of QFI corresponding to non-Hermitian sensors and prove that the effective QFI, when considering the success probability, is not larger than the total QFI of the Naimark-dilated Hermitian system. Therefore, when amounting for the neglected resources from the environment, non-Hermitian sensor cannot outperform their Hermitian counterparts, regardless of the specific form of decoherence or the choice of probe states. Our framework is applicable to various non-Hermitian sensors [13–25,34–40]. We illustrate this by analyzing three common sensing proposals, including a pseudo-Hermitian (PH) sensor and two EP-based sensors. Moreover, we show that the efficiency of non-Hermitian sensing, evaluated by the ratio of the effective OFI to the total OFI, can be optimized through postselection protocols requiring minimal experimental trials. In addition, the performance of non-Hermitian sensors versus different types of technical noises can be assessed using our framework, in accordance with previous results of postselection protocols. Our work provides a comprehensive understanding of non-Hermitian quantum sensing and is useful for exploring practical and efficient quantum metrology schemes against technical noise.

II. QUANTUM PARAMETER ESTIMATION

QPE aims to estimate an unknown parameter θ , imprinted on a quantum state ρ_{θ} . Measurements in terms of POVMs $\{\hat{E}(x)\}$ are performed on ρ_{θ} , yielding outcomes $\{x\}$ with probabilities $P(x|\theta) = \text{tr}[\rho_{\theta}\hat{E}(x)]$. For an unbiased estimator $\hat{\theta}_{\text{est}}$, the sensitivity of QPE is evaluated with its variance: $(\delta\theta)^2 \equiv \langle \hat{\theta}_{\text{est}}^2 \rangle - \langle \hat{\theta}_{\text{est}} \rangle^2$, which is lower bounded by the CRB:

$$(\delta\theta)^2 \geqslant 1/\nu F(\theta),\tag{1}$$

with ν being the repetition number of measurements [80,81]. Here,

$$F(\theta) \equiv \int dx \left[\partial_{\theta} P(x|\theta) \right]^{2} / P(x|\theta) \tag{2}$$

denotes the Fisher information (FI), and the CRB can be approximately saturated for $\nu \to \infty$. The QFI denotes the maximum FI over all possible POVMs, i.e., $F_Q(\theta) \equiv \max_{\{\hat{\mathcal{E}}(x)\}} F(\theta)$, which can be expressed with the symmetric logarithmic derivative as $F_Q(\theta) = \operatorname{tr}(\rho_\theta \hat{\mathcal{L}}_\theta^2)$, with $\hat{\mathcal{L}}$ satisfying $\partial_\theta \rho_\theta = (\rho_\theta \hat{\mathcal{L}}_\theta + \hat{\mathcal{L}}_\theta \rho_\theta)/2$ [48]. For a pure state $\rho_\theta = |\psi_\theta\rangle \langle \psi_\theta|$, the QFI can be simplified as [1,2]

$$F_Q(\theta) = 4(\langle \partial_\theta \psi_\theta | \partial_\theta \psi_\theta \rangle + |\langle \psi_\theta | \partial_\theta \psi_\theta \rangle|^2).$$
 (3)

III. POSTSELECTED MEASUREMENTS AND WEAK-VALUE AMPLIFICATION

Postselected measurements, different from ideal PVMs, have been attracting growing interest [54]. The most notable

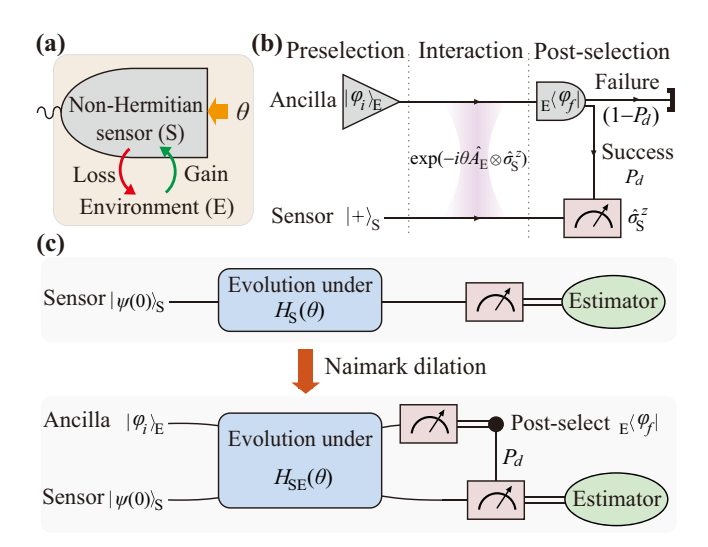


FIG. 1. (a) Non-Hermitian sensor S detects an unknown parameter θ , by coupling to an environment E with gain and/or loss. (b) Schematic of WVA, as a representative postselected measurement strategy for estimating θ . The pre- and post-selected states are $|\psi_i\rangle_{\rm E}$ and $|\psi_f\rangle_{\rm E}$, respectively, with success and rejection probabilities P_d and $(1-P_d)$, respectively. (c) Quantum circuits for the non-Hermitian sensing protocol and its Hermitian counterpart. The non-Hermitian Hamiltonian $H_{\rm SE}(\theta)$ are interconnected through the Naimark dilation theorem.

postselected detection strategy is WVA, involving a complex weak value of the observable and a small number of measurement trials [53,55]. For a simple WVA model [75] as shown in Fig. 1(b), the ancillary state is initially preselected as $|\psi_i\rangle_E$, and the sensor state is $|+\rangle_S$, where $|\pm\rangle_S$ are the eigenstates of $\hat{\sigma}^x$, with $\hat{\sigma}^{x,y,z}$ being Pauli matrices. The interaction Hamiltonian reads

$$\hat{H}_{SE} = -\theta \delta(t - t_0) \hat{\sigma}_S^z \otimes \hat{A}_E, \tag{4}$$

where θ is the interaction strength to be estimated, and $\hbar \equiv 1$. For $\theta \to 0$, the evolved joint state is approximately calculated as

$$|\Psi\rangle_{\rm SE} \simeq |+\rangle_{\rm S} \otimes |\varphi_i\rangle_{\rm E} + i\theta \hat{A}_{\rm E} |-\rangle_{\rm S} \otimes |\varphi_i\rangle_{\rm E}.$$
 (5)

By postselecting the ancilla in the state $|\varphi_f\rangle_{\rm E}$, the detected sensor state becomes

$$|\psi_d\rangle_{\rm S} \propto {}_{\rm E}\langle\varphi_f|\Psi\rangle_{\rm SE} \simeq |+\rangle_{\rm S} + \exp(i\theta A_{\rm w})|-\rangle_{\rm S},$$
 (6)

with a success probability of $P_d = |_{\rm E} \langle \varphi_f | \varphi_i \rangle_{\rm E} |^2$. Here, the weak value

$$A_{\rm w} \equiv {}_{\rm E} \langle \varphi_f | \hat{A}_{\rm E} | \varphi_i \rangle_{\rm E} / {}_{\rm E} \langle \varphi_f | \varphi_i \rangle_{\rm E} \tag{7}$$

denotes the amplification factor of the signal and grows very large when $P_d \rightarrow 0$. Although WVA seems an effective method for improving the SNR in the QPE, whether the post-selected measurements provide estimation precision superior to conventional strategies remains controversial [64–74].

Generally, a postselection process can be expressed as a PVM on the joint state $|\Psi\rangle_{SE}$:

$$\{\hat{E}_d, \hat{E}_r\} = \{|\varphi_f\rangle_{\mathsf{E}} \langle \varphi_f| \otimes \mathbb{I}_{\mathsf{S}}, (\mathbb{I}_{\mathsf{E}} - |\varphi_f\rangle_{\mathsf{E}} \langle \varphi_f|) \otimes \mathbb{I}_{\mathsf{S}}\}, \quad (8)$$

where $P_d = {}_{\rm SE}\langle\Psi|\hat{E}_d|\Psi\rangle_{\rm SE}, |\Psi_d\rangle_{\rm S} = {}_{\rm E}\langle\varphi_f|\Psi\rangle_{\rm SE}/\sqrt{P_d}$, and $\rho_{r,\rm S} \propto {\rm Tr}_{\rm E}[\hat{E}_r|\Psi\rangle_{\rm SE}\langle\Psi|]$ denote the success probability, detected state, and rejected state, respectively. The total FI for the postselection strategy, $F_{\rm tot}$, can be divided into three parts as [66]

$$F_{\text{tot}}[|\Psi\rangle_{\text{SE}}] = P_d Q_d[|\psi_d\rangle_{\text{S}}] + P_r Q_r[\rho_{r,\text{S}}] + F_{\text{post}}, \quad (9)$$

with $P_r \equiv 1 - P_d$ being the rejection probability. Here, Q_d (Q_r) denotes the QFI with respect to $|\psi_d\rangle_{\rm S}$ $(\rho_{r,{\rm S}})$, and P_dQ_d (P_rQ_r) denotes the effective QFI when considering the success (rejection) probability P_d (P_r) . The last term $F_{\rm post} \equiv (\partial_\theta P_d)^2/P_dP_r$ denotes the FI for the postselection process itself. Since the POVMs of postselected measurements may not be optimal for achieving the QFI of the joint state $|\Psi\rangle_{\rm SE}$, we have

$$F_{\text{tot}}[|\Psi\rangle_{\text{SE}}] \leqslant F_O[|\Psi\rangle_{\text{SE}}],$$
 (10)

indicating that the post-selected measurement strategy (including WVA) cannot outperform the optimal conventional strategy [66,82]. Nevertheless, the postselected strategy can be highly efficient, as P_dQ_d approaches to the total QFI, even when most of the outcomes are discarded [66,70,73].

IV. CONNECTING NON-HERMITIAN SENSING TO POSTSELECTED MEASUREMENTS WITH NAIMARK DILATION

Non-Hermitian systems have been attracting growing interest in many fields of frontier physics [46,83], among which non-Hermitian sensors are expected to have potential advantages in high-precision sensing [13–25]. Usually, quantum sensing with a non-Hermitian Hamiltonian is implemented in the open quantum system with gain and/or loss [84], and thus, the environment as a metrological resource cannot be simply neglected [see Fig. 1(a)]. Here, we apply the Naimark dilation technique [59] to extend the non-Hermitian system into a larger Hermitian one, which is widely used in quantum information theory [85,86] and feasible in experiments for simulating a non-Hermitian system [62,87].

According to the Naimark dilation theorem [61], the nonunitary evolution governed by a non-Hermitian Hamiltonian can be represented by a unitary dynamics of an enlarged system followed by a PVM, i.e., a postselection process [60,61]. For a non-Hermitian Hamiltonian $H_S(\theta)$, the evolved state $|\psi(t)\rangle_S$ is decided by the Schrödinger equation $i\partial_t |\psi(t)\rangle_S = H_S(\theta) |\psi(t)\rangle_S$. The dilated Hermitian Hamiltonian $H_{SE}(t)$ should satisfy [60]: $i\partial_t |\Psi(t)\rangle_{SE} = H_{SE}(t) |\Psi(t)\rangle_{SE}$, where

$$|\Psi(t)\rangle_{\rm SE} \propto |\psi(t)\rangle_{\rm S} \otimes |0\rangle_{\rm E} + \hat{m}(t) |\psi(t)\rangle_{\rm S} \otimes |1\rangle_{\rm E}, \quad (11)$$

 $\hat{m}(t) \equiv [\hat{\eta}(t) - \mathbb{I}]^{1/2}$ is a linear operator,

$$\hat{\eta}(t) \equiv \mathcal{T} \exp[-i \int_0^t d\tau \, H_{\rm S}^{\dagger}(\tau)] \hat{\eta}_0 \overline{\mathcal{T}} \exp[i \int_0^t d\tau \, H_{\rm S}(\tau)], \quad (12)$$

with \mathcal{T} and $\overline{\mathcal{T}}$ being the time-ordering and anti-time-ordering operators, respectively, and $|0,1\rangle$ are eigenstates of $\hat{\sigma}^z$. The dilated Hamiltonian is written as

$$H_{\rm SE}(t) = H_{\rm S}^{(1)}(t) \otimes \mathbb{I}_{\rm E} + iH_{\rm S}^{(2)}(t) \otimes \hat{\sigma}_{\rm E}^{y},$$
 (13)

where

$$H_{\rm s}^{(1)} \equiv \{H_{\rm S} + \hat{m}H_{\rm S}\hat{m} + i(\partial_t \hat{m})\hat{m}\}\hat{\eta}^{-1} \tag{14}$$

and

$$H_{\rm S}^{(2)} \equiv \{ [H_{\rm S}, \hat{m}] - i\partial_t \hat{m} \} \hat{\eta}^{-1}.$$
 (15)

The evolved state of the non-Hermitian system can be obtained from the evolution of the large Hermitian system, followed by postselecting the environment state in $|0\rangle_E$, written as $|\psi(t)\rangle_S \propto {}_E \langle 0|\Psi(t)\rangle_{SE}$.

Since $|0\rangle_E$ and $|\psi(t)\rangle_S$ correspond to the postselected state $|\varphi_f\rangle_E$ and the resulting sensor state $|\psi_d\rangle_S$ in WVA, respectively, it is reasonable that the QFI, $F_Q^{\rm nH}$, for a non-Hermitian (nH) sensor can be very large or even tends to infinity, implying an improvement of SNR. However, the environment, interacting with the non-Hermitian sensor, should be considered as an additional metrological resource, and the effective QFI, $P_dF_Q^{\rm nH}$, should be considered when analyzing the sensitivity of non-Hermitian sensors. This approach is similar to neglecting some detection trials in the postselected detection strategy. Using Eqs. (9) and (10), we conclude that the effective QFI for non-Hermitian sensors does not exceed the QFI of their dilated Hermitian counterparts as

$$P_d F_O^{\text{nH}}[|\psi(t)\rangle_{\text{S}}] \leqslant F_Q[|\Psi(t)\rangle_{\text{SE}}],\tag{16}$$

with $P_d = \text{Tr}_S[_E \langle 0 | \Psi \rangle_{SE} \langle \Psi | 0 \rangle_E]$. Note that our results also hold for non-Hermitian sensors with experimental imperfections on the detectors that can be expressed as quantum channels, by considering of the noisy QFI [50,51].

In addition to the ultimate sensitivity limits, mapping non-Hermitian sensing to a postselection QPE strategy offers a perspective for comparing the efficiencies of different types of non-Hermitian sensors. Similar to WVA, the efficiency can be evaluated by comparing the effective QFI, $P_d F_Q^{\rm nH}$, with the total QFI, F_Q , for the dilated Hermitian system. When the ratio $P_d F_Q^{\rm nH}/F_Q \rightarrow 1$ with a small value of P_d , it indicates a highly efficient non-Hermitian sensing scheme, in analog with the advantage of "when less is more" in WVA [71]. Next, we investigate different types of non-Hermitian sensors from the perspective of postselected measurements.

V. PSEUDO-HERMITIAN SENSOR

We first consider a pH sensor with a Hamiltonian for $\lambda \in (0,1]:$

$$H_{\rm S}^{\rm pH} = \theta \begin{pmatrix} 0 & \lambda^{-1} \\ \lambda & 0 \end{pmatrix}, \tag{17}$$

which was believed to enable non-Hermiticity-enhanced sensing [39,40]. Here, θ is the unknown parameter to be estimated, and H_S^{pH} is non-Hermitian when $\lambda \neq 1$. By setting $|0\rangle_S$ as the initial state, the time-evolved state under H_S^{pH} is

$$|\psi(t)\rangle_{S} = [\cos(\theta t) |0\rangle_{S} - i\lambda \sin(\theta t) |1\rangle_{S}]/C,$$
 (18)

with $C \equiv [\cos^2(\theta t) + \lambda^2 \sin^2(\theta t)]^{1/2}$, and the QFI with respect to $|\psi(t)\rangle_S$ is calculated as

$$F_Q^{\text{pH}}[|\psi(t)\rangle_{\text{S}}] = 4\lambda^2 t^2 / C^4. \tag{19}$$

The QFI under the non-Hermitian condition ($\lambda \neq 1$) is larger than that for the Hermitian case ($\lambda = 1$), when choosing a

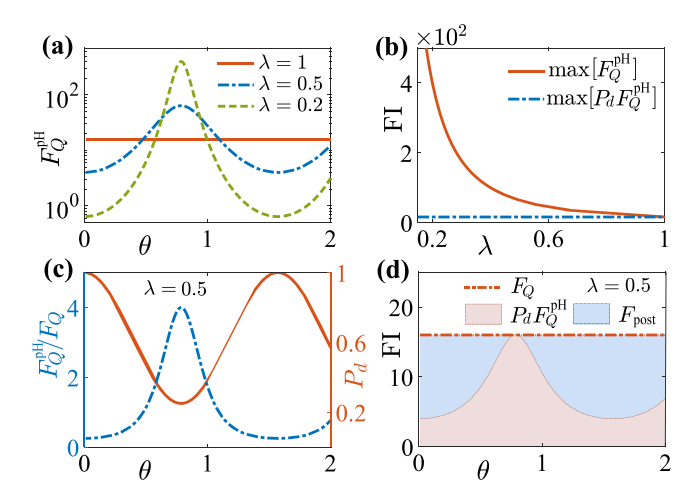


FIG. 2. Pseudo-Hermitian sensor with the Hamiltonian (17). (a) QFI, $F_Q^{\rm PH}$, for the sensor state $|\psi(t)\rangle_{\rm S}$ for $\lambda=1,\,0.5,\,0.2$, when t=2. (b) The maximum $F_Q^{\rm PH}$ over θ diverges as $\lambda\to 0$. However, the maximum effective QFI, $P_dF_Q^{\rm PH}$, becomes finite for any value of λ , with the success probability P_d . (c) Ratio of the pseudo-Hermitian QFI over the total QFI for the dilated system $F_Q^{\rm PH}/F_Q$ (blue dashdotted curve) is shown with the success probability P_d (red solid curve) for $\lambda=0.5$. (d) The total QFI of the extended system, F_Q , the effective QFI, P_dQ_d , and the FI of the postselection process, $F_{\rm post}$, for $\lambda=0.5$. Here, the effective QFI for the rejected state vanishes $P_rQ_r=0$, since $\partial_\theta |\psi_r(t)\rangle_{\rm S}=0$.

proper parameter range of θ , e.g., see Fig. 2(a) for t=2. Moreover, the maximum QFI, $\max_{\theta} \{F_Q^{\text{pH}}\}$, diverges as $\lambda \to 0$; see Fig. 2(b), since it is proportional to λ^{-2} , implying superior performance to the conventional Hermitian case.

The Naimark-dilated Hermitian Hamiltonian with respect to the pseudo-Hermitian system (17) can be obtained as

$$H_{\rm SE} = \theta \lambda (\hat{\sigma}_{\rm S}^x \otimes \mathbb{I}_{\rm E} - \sqrt{\lambda^{-2} - 1} \hat{\sigma}_{\rm S}^y \otimes \hat{\sigma}_{\rm E}^y). \tag{20}$$

The time-evolved state of the extended system is

$$|\Psi(t)\rangle_{SE} = |\psi(t)\rangle_{S} \otimes |0\rangle_{E} + i(1 - \lambda^{2})^{1/2} \sin(\theta t) |1\rangle_{S} \otimes |1\rangle_{E},$$
(21)

which is initialized at $|\Psi(0)\rangle_{\rm SE} = |0\rangle_{\rm S} \otimes |0\rangle_{\rm E}$. After post-selecting, the environment in $|0\rangle_{\rm E}$ with a success probability of $P_d = [(1-\lambda^2)\sin^2(\theta t)+1]^{-1}$, the time-evolved sensor state $|\psi(t)\rangle_{\rm S}$ is obtained. For some values of θ , $F_Q^{\rm pH}[|\psi\rangle_{\rm S}]/F_Q[|\Psi\rangle_{\rm SE}] > 1$ [see Fig. 2(c)], where P_d becomes relatively small. Here, the effective QFI, $P_d F_Q^{\rm pH}$, should be considered, which does not diverge [see Fig. 2(b)]. Using Eq. (9), we have $F_Q \geqslant F_{\rm tot} \geqslant P_d F_Q^{\rm pH}$, as shown in Fig. 2(d), indicating that the pseudo-Hermitian sensor is suboptimal when compared to its dilated Hermitian counterpart.

Furthermore, Fig. 2(d) shows that $P_d F_Q^{\rm pH} \approx F_Q$, as $\theta \simeq 0.785$, indicating that the pseudo-Hermitian sensor can be efficient. It is because that most information about θ can be obtained with very few measurement trials on the detected state, which, similar to WVA, could help to overcome some technical noise [40,67,71]. In addition, since the rejected state does not contain information about θ , it is straightforward that $Q_r = 0$.

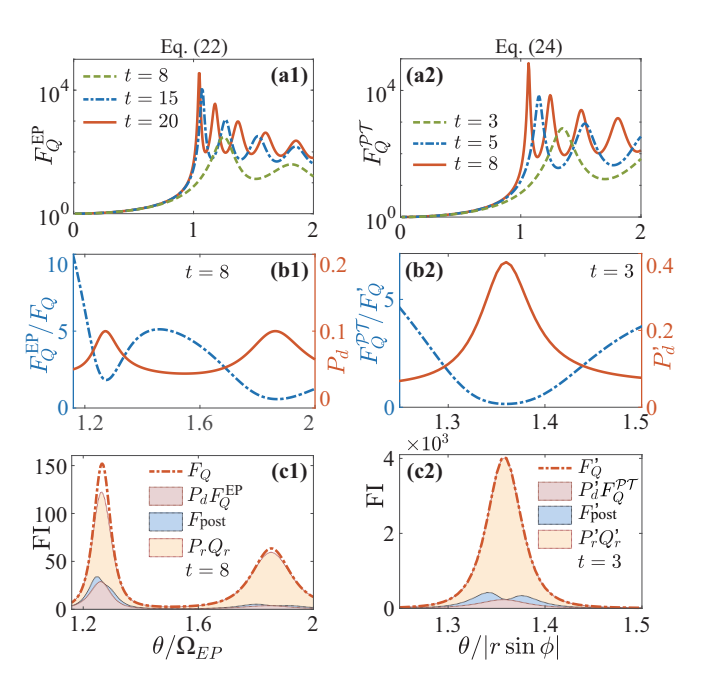


FIG. 3. Two EP-based sensors with Hamiltonians in Eqs. (22) and (24), respectively. (a1) QFI, $F_Q^{\rm EP}$, for the EP-based sensor (22) for evolution times t=8, 15, 20, when choosing $\Omega_{\rm EP}=\omega_{\rm ccw}$. (a2) QFI, $F_Q^{\mathcal{PT}}$, for the EP-based sensor (24) for t=3, 5, 8, with $\phi=\pi/4$. (b1) and (b2) Ratios of the QFI for the EP-based sensors $F_Q^{\rm EP}$ and $F_Q^{\mathcal{PT}}$ to the total QFI F_Q and F_Q' for the extended systems (blue dashed-dotted curves) are shown with the corresponding success probabilities P_d and P_d' , respectively. (c1) and (c2) The total effective QFI, the effective QFI of EP-based sensors $P_dF_Q^{\rm EP}$ and $P_d'F_Q^{\mathcal{PT}}$, the effective QFI for the rejected states $P_Q'Q_T'$ and $P_Q'Q_T'$, and the FI for postselection process $F_{\rm post}$ and $F_{\rm post}'$ are shown for t=8 and 3, respectively.

VI. TWO TYPES OF EP-BASED NON-HERMITIAN SENSORS

In non-Hermitian systems with EPs, where gain and loss can be perfectly balanced, exotic behaviors are predicted to occur [47,83,88] with promising applications, e.g., EP-based sensing [14,15,31,41]. Here, we consider two types of EP-based sensors without and with \mathcal{PT} symmetry, respectively.

The first model has a non-Hermitian Hamiltonian:

$$\hat{H}_{\rm S}^{\rm EP} = \begin{pmatrix} \omega_{\rm cw} & i\Omega_{\rm EP}/2\\ i\Omega_{\rm EP}/2 & \omega_{\rm ccw} \end{pmatrix},\tag{22}$$

which has been experimentally realized in a Brillouin ring laser gyroscope [15,31]. This EP-based sensor estimates the frequency difference $\theta \equiv \omega_{\rm cw} - \omega_{\rm ccw}$ by measuring the eigenenergy difference ΔE of the Hamiltonian in Eq. (22). The eigenenergies of $\hat{H}_{\rm S}^{\rm EP}$ are $E_{\pm} \equiv [\omega_{\rm cw} + \omega_{\rm ccw} \pm (\theta^2 - \Omega_{\rm EP}^2)^{1/2}]/2$, with $\Delta E = (\theta^2 - \Omega_{\rm EP}^2)^{1/2}$, which vanishes at two EPs ($\theta = \pm \Omega_{\rm EP}$). The estimation sensitivity $\delta \theta$ is proportional to the inverse differential $(\partial \Delta E/\partial \theta)^{-1}$, and the differential diverges at EPs, implying highly sensitive estimation in absence of noise [15]. For the initial state $|0\rangle_{\rm S}$, as time becomes sufficiently long, the QFI diverges near the EPs [see Fig. 3(a)]. Then, we consider the dilated Hamiltonian $\hat{H}_{\rm SE}^{\rm EP}(t)$ using Eq. (13) (see Appendix B for more details). For the

initial state

$$|\Psi(0)\rangle_{SE} = |0\rangle_{S} \otimes |0\rangle_{E} + [\hat{\eta}(0) - \mathbb{I}]^{1/2} |0\rangle_{S} \otimes |1\rangle_{E}, \quad (23)$$

the time-evolved state satisfies $i\partial_t |\Psi(t)\rangle_{\rm SE}^{\rm EP} = \hat{H}_{\rm SE}^{\rm EP}(t) |\Psi(t)\rangle_{\rm SE}$. Without loss of generality, we set $\hat{\eta}_0 = 100 \cdot \hat{\mathbb{I}}$ for $t \leqslant 15$ and calculate the QFI for the EP-based and the extended Hermitian sensors, respectively, which are compared to the success probability P_d in Fig. 3(b1). Figure 3(c1) shows that the effective QFI for this EP-based sensor is much smaller than the QFI for the dilated Hermitian system as $P_d F_Q^{\rm EP} \leqslant F_Q$, which complies with Eq. (16). It demonstrates that the EP-based sensor (22) cannot outperform the conventional Hermitian sensor.

Next, we consider a two-level \mathcal{PT} -symmetric system [14] with a Hamiltonian:

$$\hat{H}_{S}^{\mathcal{PT}} = \begin{pmatrix} re^{i\phi} & \theta \\ \theta & re^{-i\phi} \end{pmatrix}, \tag{24}$$

where θ is the unknown parameter to be estimated. Its eigenvalues are $E_{\pm}=r\cos\phi\pm(\theta^2-r^2\sin^2\phi)^{1/2}$, and this \mathcal{PT} -symmetric system has two EPs $(\theta=\pm r\sin\phi)$. When $|\theta|>|r\sin\phi|$, the eigenvalues are real; otherwise, the eigenvalues are complex since the \mathcal{PT} symmetry is broken [29,47,89]. Similarly, a highly sensitive sensor is theoretically predicted near the EPs, due to the divergence of the inverse differential $(\partial\Delta E/\partial\theta)^{-1}$, where the QFI can be arbitrary large for $t\to\infty$ {see Fig. 3(a2)]. Considering the postselection on the dilated Hermitian system, the effective QFI of the \mathcal{PT} -symmetric sensor is also smaller than the total QFI as $P_d'F_Q^{\mathcal{PT}}\leqslant F_Q'$ [see Fig. 3(c2)]. Therefore, by relating EP-based sensing to postselected

Therefore, by relating EP-based sensing to postselected measurements, both EP-based sensors cannot outperform their extended Hermitian counterparts even with divergent QFI near EPs. Moreover, the maximum effective QFI appear when the success probabilities P_d and P'_d achieve their local maxima [see Figs. 3(b1) and 3(b2)]. In the context of postselected measurements, it corresponds to an inefficient postselection strategy, since "when more is less." In comparison, the effective QFI for the pseudo-Hermitian sensor achieves the maximum when the success probability achieves its local minimum [Fig. 3(c2)], i.e., "when less is more." Another EP-based sensing scheme [25], where the dynamics of a loss-loss system is mathematically equivalent to that of a gain-loss system apart from a global exponential decay, is discussed in Appendix F.

VII. CONCLUSIONS AND DISCUSSIONS

In summary, by employing the Naimark dilation method, we establish a connection between non-Hermitian quantum sensing and a postselection process implemented on an extended Hermitian system. Through analyzing the effective QFI of the non-Hermitian sensing from the perspective of postselected measurements, we demonstrate that non-Hermitian sensors exhibit suboptimal performance compared to their extended Hermitian counterparts, when all information is harnessed. Analogous to WVA, the efficiency of non-Hermitian quantum sensing, quantified by the ratio of the effective QFI to the total QFI, can be optimized under post-selected measurement protocols with minimal experimental

trials. Our work establishes an alternative framework for understanding non-Hermitian sensing from the perspective of postselected measurements and facilitates the design of robust quantum metrological protocols against technical noise.

Note that our results based on the conservation of total QFI do not mean that non-Hermitian sensing is completely ineffective. Several implementations exhibit enhanced parameter sensitivity under specific conditions [25,40]. First, since full control of the sensor-environment system and the extraction of all information from the environment space is experimentally infeasible, non-Hermitian sensing provides a practical method to harness useful quantum metrological resources from the interaction with the environment. In addition, the Naimark dilation method may not be the minimal extension of the system [90], but fortunately, in most experiments, the environmental dimension is much larger than the Naimark-dilated ancillary system dimension. Then, the efficiency of non-Hermitian sensors can be evaluated using our framework. For instance, the pseudo-Hermitian sensor (17) relates to the postselection protocol that requires very few trials of measurements and has an effective OFI that equals the total OFI, showing potential advantages when the control of the environment is limited. Since postselection detection protocols can suppress some forms of technical noise [65,67,91], our theoretical framework will further motivate the design of practical noise-resilient quantum metrology that leverages the interaction with the environment as a resource rather than a limitation. Further research on this topic would include the use of the quantum correlation measurement [92,93] to remove the classical noise and practical QPE with different statistical methods, e.g., the maximum likelihood analysis [94] and Bayesian analysis [95].

ACKNOWLEDGMENTS

We would like to thank Qing Ai for useful discussions. T.L. acknowledges the support from the National Natural Science Foundation of China (Grant No. 12274142), the Key Program of the National Natural Science Foundation of China (Grant No. 62434009), the Fundamental Research Funds for the Central Universities (Grant No. 2023ZYGXZR020), the Introduced Innovative Team Project of Guangdong Pearl River Talents Program (Grant No. 2021ZT09Z109), and the Startup Grant of South China University of Technology (Grant No. 20210012). K.X. was partly supported by the National Natural Science Foundation of China (Grant No. 92365107), the National Key R&D Program of China (Grant No. 2019YFA0308700), the Program for Innovative Talents and Teams in Jiangsu (Grant No. JSSCTD202138), and the National University of Defense Technology Independent Innovation Science Foundation (Grant No. 24-ZZCX-JDZ-11). Y.-R.Z. was supported in part by the National Natural Science Foundation of China (Grant No. 12475017), the Natural Science Foundation of Guangdong Province (Grant No. 2024A1515010398), and the Startup Grant of South China University of Technology (Grant No. 20240061). F.N. was supported in part by the Japan Science and Technology Agency (JST) [via the CREST Quantum Frontiers program Grant No. JPMJCR24I2, the Quantum Leap Flagship Program (Q-LEAP), and the Moonshot R&D Grant No. JPMJMS2061].

DATA AVAILABILITY

The data that support the findings of this article are openly available [96].

APPENDIX A: TOTAL FISHER INFORMATION FOR THE POSTSELECTION PROCESS

Here, we analyze the total Fisher information for the post-selection process. For the postselected measurement on the joint state $|\Psi\rangle_{\rm SE}$, the success probabilities of obtaining the detected state $|\psi_d\rangle_{\rm S}$ and the rejected state $\rho_{\rm S}^r$ are P_d and $P_r\equiv 1-P_d$, respectively. Subsequent measurements on the sensor state yield outcomes x with probabilities p(x|d) and p(x|r) for the detected and rejected states, respectively. The total Fisher information for the postselection process can be calculated as

$$F_{\text{tot}} = \int dx \frac{[\partial_{\theta} P_{d} p(x|d)]^{2}}{P_{d} p(x|d)} + \int dx \frac{[\partial_{\theta} P_{r} p(x|r)]^{2}}{P_{r} p(x|r)}$$
$$= P_{d} \int dx \frac{[\partial_{\theta} p(x|d)]^{2}}{p(x|d)} + P_{r} \int dx \frac{[\partial_{\theta} p(x|r)]^{2}}{p(x|r)} + \sum_{i=d,r} \frac{(\partial_{\theta} P_{i})^{2}}{P_{i}}$$

$$= P_d F_d + P_r F_r + F_{\text{post}}.$$
 (A1)

Here, F_d and F_r represent the Fisher information for $|\psi_d\rangle_S$ and ρ_S^r , respectively, and F_{post} denotes the Fisher information for the postselection process itself.

In the ideal case, where the POVMs $\{\hat{E}_d\}$ and $\{\hat{E}_r\}$ performed on the detected and rejected states, respectively, are assumed to be optimal, the total Fisher information F_{tot} for the postselection process can be optimized as [66]

$$F_{\text{tot}}^{\text{opt}}[|\Psi\rangle_{\text{SE}}] \equiv \max_{\{\hat{E}_d\}} \max_{\{\hat{E}_r\}} F_{\text{tot}}$$
(A2)

$$= P_d Q_d[|\psi_d\rangle_S] + P_r Q_r[\rho_{r,S}] + F_p, \quad (A3)$$

where Q_d and Q_r denote the quantum Fisher information of $|\psi_d\rangle_S$ and $\rho_{r,S}$, respectively.

APPENDIX B: NAIMARK DILATION OF NON-HERMITIAN HAMILTONIANS

Under the impact of a non-Hermitian Hamiltonian $H_S(t)$, the time-evolved state $|\psi(t)\rangle_S$ is governed by the Schrödinger equation with $\hbar \equiv 1$ as

$$i\partial_t |\psi(t)\rangle_{S} = H_{S}(t) |\psi(t)\rangle_{S}.$$
 (B1)

According to the Naimark dilation theorem [58,59], this nonunitary dynamics can be equivalently represented as the dynamics of an extended system-environment Hermitian system followed by postselection. The time evolution with the dilated Hermitian Hamiltonian $H_{SE}(t)$ satisfies

$$i\partial_t |\Psi(t)\rangle_{\rm SE} = H_{\rm SE}(t) |\Psi(t)\rangle_{\rm SE}.$$
 (B2)

The joint state $|\Psi(t)\rangle_{SE}$ evolves as

$$|\Psi(t)\rangle_{SE} \propto |\psi(t)\rangle_{S} \otimes |0\rangle_{E} + \hat{m}(t) |\psi(t)\rangle_{S} \otimes |1\rangle_{E},$$
 (B3)

where $\hat{m}(t)$ is a linear time-dependent operator, $|0\rangle$ and $|1\rangle$ are eigenstates of σ^z , with $\hat{\sigma}^{x,y,z}$ being Pauli matrices.

Without loss of generality, $H_{SE}(t)$ can be written as

$$H_{SE}(t) = \left(\begin{array}{c|c} H_{S}^{(1)}(t) & H_{S}^{(2)}(t) \\ \hline H_{S}^{(2)\dagger}(t) & H_{S}^{(4)}(t) \end{array}\right), \tag{B4}$$

where $H_{\rm S}^{(1)}(t)$ and $H_{\rm S}^{(4)}(t)$ are Hermitian. By substituting Eqs. (B1) and (B4) into Eq. (B2), we have

$$H_{\rm S}^{(1)}(t) + H_{\rm S}^{(2)}(t)\hat{m}(t) - H_{\rm S}(t) = 0,$$
 (B5)

$$H_{\rm S}^{(2)\dagger}(t) + H_{\rm S}^{(4)}(t)\hat{m}(t) - \hat{m}(t)H_{\rm S}(t) - i\partial_t\hat{m}(t) = 0.$$
 (B6)

The Hermitian conjugate of these equations gives

$$H_{\rm s}^{(1)}(t) + \hat{m}(t)^{\dagger} H_{\rm s}^{(2)}(t)^{\dagger} - H_{\rm S}(t)^{\dagger} = 0,$$
 (B7)

$$H_{\rm S}^{(2)}(t) + \hat{m}(t)^{\dagger} H_{\rm S}^{(4)}(t) - H_{\rm S}(t)^{\dagger} \hat{m}(t)^{\dagger} + i \partial_t \hat{m}(t)^{\dagger} = 0.$$
(B8)

The unitary time evolution of the extended Hermitian system requires

$$\partial_{tSE} \langle \Psi(t) | \Psi(t) \rangle_{SE} = 0,$$
 (B9)

which can be calculated as

$$0 = \frac{\partial}{\partial t} \mathbf{S} \langle \psi(t) | [\hat{m}(t)^{\dagger} \hat{m}(t) + \mathbb{I}] | \psi(t) \rangle_{\mathbf{S}}$$

= $\mathbf{S} \langle \psi(t) | i [H_{\mathbf{S}}(t)^{\dagger} \hat{\eta}(t) - \hat{\eta}(t) H_{\mathbf{S}}(t) - i \partial_t \hat{\eta}(t)] | \psi(t) \rangle_{\mathbf{S}},$

where we have defined $\hat{\eta}(t) \equiv \hat{m}^{\dagger}(t)\hat{m}(t) + \hat{\mathbb{I}}$. We further have

$$H_{\mathcal{S}}^{\dagger}(t)\hat{\eta}(t) - \hat{\eta}(t)H_{\mathcal{S}}(t) - i\partial_t\hat{\eta}(t) = 0$$
 (B10)

and the solution takes the form

$$\hat{\eta}(t) = \mathcal{T}e^{-i\int_0^t d\tau H_{S}(\tau)^{\dagger}} \hat{\eta}(0) \overline{\mathcal{T}}e^{i\int_0^t d\tau H_{S}(\tau)}, \tag{B11}$$

with \mathcal{T} and $\overline{\mathcal{T}}$ being time-ordering operator and anti-time-ordering operator, respectively. Note that the form of $\hat{\eta}(0)$ is indeterminate. The operator $\hat{m}(t)$ is given by

$$\hat{m}(t) = \hat{U}[\hat{\eta}(t) - \mathbb{I}]^{\frac{1}{2}},\tag{B12}$$

where \hat{U} is an arbitrary unitary operator. For simplicity, we set $\hat{U} = \mathbb{I}$, and Eq. (B12) becomes

$$\hat{m}(t) = \left[\hat{\eta}(t) - \mathbb{I}\right]^{\frac{1}{2}}.\tag{B13}$$

In addition, it is required to choose an appropriate Hermitian $\hat{\eta}(0)$ to keep $[\hat{\eta}(t) - \mathbb{I}]$ a positive operator (see Appendix C for details) such that $\hat{m}(t)$ is Hermitian. By using Eqs. (B5)–(B8), one possible solution for Eq. (B4) can be obtained as [62]

$$H_{S}^{(1)}(t) = H_{S}^{(4)}(t) = \{H_{S} + \hat{m}H_{S}\hat{m} + i(\partial_{t}\hat{m})\hat{m}\}\hat{\eta}^{-1},$$

$$H_{S}^{(2)}(t) = -H_{S}^{(2)}(t)^{\dagger} = \{[H_{S}, \hat{m}] - i\partial_{t}\hat{m}\}\hat{\eta}^{-1}.$$
 (B14)

After some calculations, the extended Hamiltonian can be written as

$$H_{\rm SE}(t) = H_{\rm S}^{(1)}(t) \otimes \mathbb{I}_{\rm E} + iH_{\rm S}^{(2)}(t) \otimes \hat{\sigma}_{\rm E}^{y}.$$
 (B15)

Next, H called as a ζ -pseudo-Hermitian Hamiltonian *iff* there exists a Hermitian operator $\hat{\zeta}$, satisfying

$$\hat{\zeta}H^{\dagger} = H\hat{\zeta}. \tag{B16}$$

Assuming that H_S is a time-independent ζ -pseudo-Hermitian Hamiltonian, we can simplify the Naimark dilation by choosing a positive $\hat{\zeta}$. We let $\hat{\eta}(0) = \hat{\zeta}/\nu_{\zeta}$, where ν_{ζ} is the minimum eigenvalue of $\hat{\zeta}$. Here, $\hat{\eta}$ can be obtained with Eq. (B11) as

$$\hat{\eta}(t) = e^{-iH_S^{\dagger}t} \hat{\eta}(0)e^{iH_St} = \hat{\eta}(0).$$
 (B17)

Here, $\hat{\eta} = \hat{\zeta}/\nu_{\zeta}$ and $\hat{m} = [\hat{\eta} - \mathbb{I}]^{1/2}$ are both time-independent in this case. Thus, Eq. (B14) can be simplified as

$$H_{\rm S}^{(1)} = H_{\rm S}^{(4)} = (H_{\rm S} + \hat{m}H_{\rm S}\hat{m})\hat{\eta}^{-1},$$

 $H_{\rm S}^{(2)} = -H_{\rm S}^{(2)\dagger} = [H_{\rm S}, \hat{m}]\hat{\eta}^{-1},$ (B18)

where the extended Hamiltonian H_{SE} expressed in Eq. (B15) is also time independent.

APPENDIX C: UNIVERSALITY OF NAIMARK DILATION METHOD

To ensure $\hat{m}(t) = [\hat{\eta}(t) - \mathbb{I}]^{\frac{1}{2}}$ to be Hermitian, we need to choose appropriate $\hat{\eta}(0)$ to keep $\hat{\eta}(t) - \mathbb{I}$ positive. First, we choose an arbitrary positive operator

$$\hat{\eta}'(0) = \hat{\gamma}^{\dagger} \hat{\gamma}. \tag{C1}$$

By using Eq. (B11), we have

$$\hat{\eta}'(t) = \left[\hat{\gamma} \overline{\mathcal{T}} e^{i \int_0^t d\tau \, H_{\mathcal{S}}(\tau)}\right]^{\dagger} \left[\hat{\gamma} \overline{\mathcal{T}} e^{i \int_0^t d\tau \, H_{\mathcal{S}}(\tau)}\right], \quad (C2)$$

which is still positive. By supposing the minimal eigenvalue of $\hat{\eta}'(t)$ is ν' and defining

$$\hat{\eta}(0) \equiv \frac{\hat{\eta}'(0)}{v'},\tag{C3}$$

we ensure that

$$\hat{\eta}(t) - \mathbb{I} = \mathcal{T}e^{-i\int_0^t d\tau \, H_{\mathcal{S}}(\tau)^{\dagger}} \hat{\eta}(0)\overline{\mathcal{T}}e^{i\int_0^t d\tau \, H_{\mathcal{S}}(\tau)} - \mathbb{I}$$
 (C4)

is positive, for the saturation of a Hermitian $\hat{m}(t)$.

APPENDIX D: DILATION OF PSEUDO-HERMITIAN HAMILTONIAN

The pseudo-Hermitian Hamiltonian is written as

$$H_{\rm S}^{\rm pH} = \theta \begin{pmatrix} 0 & \lambda^{-1} \\ \lambda & 0 \end{pmatrix},$$
 (D1)

where $\lambda \in (0,1]$, and θ is the unknown parameter to be estimated. The Hamiltonian H_S^{pH} is non-Hermitian when $\lambda \neq 1$. By setting $|0\rangle_S$ as the initial state, the time-evolved state under the impact of H_S^{pH} is calculated as

$$|\psi(t)\rangle_{S} = \frac{\exp\left(-iH_{S}^{pH}t\right)|0\rangle_{S}}{\operatorname{tr}\left[\langle\psi(0)|\exp\left(iH_{S}^{pH\dagger}t\right)\exp\left(-iH_{S}^{pH}t\right)|\psi(0)\rangle\right]^{1/2}}$$
$$= [\cos(\theta t)|0\rangle_{S} - i\lambda\sin(\theta t)|1\rangle_{S}]/C, \qquad (D2)$$

with $C \equiv [\cos^2(\theta t) + \lambda^2 \sin^2(\theta t)]^{1/2}$ is the normalization coefficient. The quantum Fisher information for a pure state $|\psi_{\theta}\rangle$

can be expressed as $F_Q(\theta) = 4(\langle \partial_\theta \psi_\theta | \partial_\theta \psi_\theta \rangle + |\langle \psi_\theta | \partial_\theta \psi_\theta \rangle|^2)$ [1,2]. We calculate the quantum Fisher information for $|\psi(t)\rangle_S$ as

$$F_{\mathcal{Q}}[|\psi(t)\rangle_{S}] = \frac{4\lambda^{2}t^{2}}{C^{4}}.$$
 (D3)

With the Naimark dilation method as discussed in Appendix B, a unitary dynamics of an enlarged system can be used to equivalently represent the dynamics of this pseudo-Hermitian system. Thus, we can construct an appropriate extended system by using the time-independent dilation method (see Appendix B for more details). Here, $H_{\rm S}^{\rm pH}$ is a η -pseudo-Hermitian Hamiltonian, satisfying

$$H_{\rm S}^{\rm pH\dagger} \hat{\eta} = \hat{\eta} H_{\rm S}^{\rm pH}.$$
 (D4)

The Hermitian operator $\hat{\eta}$ is calculated as

$$\hat{\eta} = \begin{pmatrix} 1 & a \\ a & \lambda^{-2} \end{pmatrix}, \tag{D5}$$

with a being an arbitrary real number. Without loss of generality, we set a=0, and the operator $\hat{\eta}$ is given by

$$\hat{\eta} = \begin{pmatrix} 1 & 0 \\ 0 & \lambda^{-2} \end{pmatrix}. \tag{D6}$$

Here, $(\hat{\eta} - \mathbb{I})$ is positive. With Eq. (B12), \hat{m} can be written as

$$\hat{m} = \begin{pmatrix} 0 & 0 \\ 0 & \sqrt{\lambda^{-2} - 1} \end{pmatrix}. \tag{D7}$$

With Eq. (B18), $H_S^{(1)}$ and $H_S^{(2)}$ are calculated as

$$H_{S}^{(1)} = \theta \lambda \hat{\sigma}_{S}^{x},$$

$$H_{S}^{(2)} = i\theta \lambda \sqrt{\lambda^{-2} - 1} \hat{\sigma}_{S}^{y}.$$
 (D8)

Taking Eq. (D8) into Eq. (B15), the dilated Hamiltonian reads

$$H_{\rm SE} = \theta \lambda \left(\hat{\sigma}_{\rm S}^{x} \otimes \hat{\mathbb{I}}_{\rm E} - \sqrt{\lambda^{-2} - 1} \hat{\sigma}_{\rm S}^{y} \otimes \hat{\sigma}_{\rm E}^{y} \right). \tag{D9}$$

The initial extended state is chosen as

$$\begin{split} |\Psi(0)\rangle_{\mathrm{SE}} &\propto |0\rangle_{\mathrm{S}} \otimes |0\rangle_{\mathrm{E}} + \hat{m} |0\rangle_{\mathrm{S}} \otimes |1\rangle_{\mathrm{E}} \\ &= |0\rangle_{\mathrm{S}} \otimes |0\rangle_{\mathrm{E}} \,, \end{split} \tag{D10}$$

and the time evolution of the extended system is governed by \hat{H}_{SF} as

$$|\Psi(t)\rangle_{SE} = e^{-i\hat{H}_{SE}t} |\Psi(0)\rangle_{SE}$$
 (D11)

$$= |\psi(t)\rangle_{S} \otimes |0\rangle_{E} + \hat{m} |\psi(t)\rangle_{S} \otimes |1\rangle_{E}$$
 (D12)

$$= |\psi(t)\rangle_{S} \otimes |0\rangle_{E} + i\sqrt{1 - \lambda^{2}} \sin(\theta t) |1\rangle_{S} \otimes |1\rangle_{E}.$$
(D13)

Therefore, by postselecting the corresponding environment state in $|0\rangle_E$, the evolved state of the pseudo-Hermitian system can be equivalently obtained as

$$|\psi(t)\rangle_{S} \propto {}_{E}\langle 0|\Psi(t)\rangle_{SE}.$$
 (D14)

APPENDIX E: DILATION OF HAMILTONIANS OF TWO EXCEPTIONAL-POINT-BASED SENSORS

Here, we show more details for two examples of exceptional-point-based sensors. One model involves a non-Hermitian Hamiltonian that is written as

$$H_{\rm S}^{\rm EP} = \begin{pmatrix} \omega_{\rm cw} & i\Omega_{\rm EP}/2 \\ i\Omega_{\rm EP}/2 & \omega_{\rm ccw} \end{pmatrix},$$
 (E1)

where $\theta \equiv \omega_{\rm cw} - \omega_{\rm ccw}$ is the parameter to be estimated. Two eigenenergies of $H_{\rm S}^{\rm EP}$ are

$$E_{\pm} \equiv \left[\omega_{\text{cw}} + \omega_{\text{ccw}} \pm \left(\theta^2 - \Omega_{\text{EP}}^2\right)^{1/2}\right]/2, \tag{E2}$$

with $\Delta E = (\theta^2 - \Omega_{\rm EP}^2)^{1/2}$. Setting $|0\rangle_{\rm S}$ as the initial state, the evolved state reads

$$|\psi(t)\rangle_{S} = \left[\left(\Delta E \cos \frac{\Delta E t}{2} - i\theta \sin \frac{\Delta E t}{2} \right) |0\rangle_{S} + \sin \frac{\Delta E t}{2} |1\rangle_{S} \right] / C_{1}, \tag{E3}$$

where $C_1 = (\theta^2 - \cos \Delta E t)^{1/2}$ is the normalization coefficient. The quantum Fisher information for the state $|\psi(t)\rangle_S$ diverges near two exceptional points for $t \to \infty$ [see Fig. 4(a1)].

Then, we use the dilation method to extend the above non-Hermitian system to a large Hermitian one. With Eq. (B15), we can obtain the extended Hermitian Hamiltonian H_{SE} , and the extended system is initialized at

$$|\Psi(0)\rangle_{SE} = |\psi(t)\rangle_{S} \otimes |0\rangle_{E} + \hat{m}(t) |\psi(t)\rangle_{S} \otimes |1\rangle_{E}.$$
 (E4)

From a perspective of postselected measurements, the evolved state of the non-Hermitian system $|\psi(t)\rangle_{\rm S}$ is the detected state $|\psi_d\rangle_{\rm S} \equiv |\psi(t)\rangle_{\rm S} \propto {}_{\rm E}\langle 0|\Psi(t)\rangle_{\rm SE}$, with $|\Psi(t)\rangle_{\rm SE}$ and $|0\rangle_{\rm E}$ being the joint state and the postselection state, respectively. The rejected state is $|\psi_r\rangle_{\rm S} \propto {}_{\rm E}\langle 1|\Psi(t)\rangle_{\rm SE}$. Then, we calculate the total quantum Fisher information $F_Q[|\Psi\rangle_{\rm SE}]$ for the extended state, the effective quantum Fisher information $P_dF_Q^{\rm EP}$ and P_rQ_r for the detected and rejected states, respectively, and the Fisher information $F_{\rm post}$ for postselection process itself [see Fig. 4(b1)].

The other model describes a two-level \mathcal{PT} -symmetric system with a Hamiltonian [14]:

$$H_{\rm S}^{\mathcal{PT}} = \begin{pmatrix} re^{i\phi} & \theta \\ \theta & re^{-i\phi} \end{pmatrix},$$
 (E5)

where θ is the parameter to be estimated. Setting $|0\rangle_S$ as the initial state and $\phi = \pi/4$, the evoluted state reads

$$|\psi(t)\rangle_{S} = \left[\left(\frac{\Delta E}{2} \cos \frac{\Delta E t}{2} - \frac{\sqrt{2}}{2} r \sin \frac{\Delta E t}{2} \right) |0\rangle_{S} -i \sin \frac{\Delta E t}{2} |1\rangle_{S} \right] / C_{2}, \tag{E6}$$

with $\Delta E = (\theta^2 - r^2/2)^{1/2}$. We calculate the quantum Fisher information $F_Q^{\mathcal{P}^{\mathcal{T}}}[|\psi\rangle_S]$ as shown in Fig. 4(a2), and then consider the dilation of the $\mathcal{P}\mathcal{T}$ -symmetric system. Similarly, we calculate the total quantum Fisher information $F_Q'[|\Psi\rangle_{SE}]$, the effective quantum Fisher information for the detected state $P_d'F_Q^{\mathcal{P}^{\mathcal{T}}}$, the effective quantum Fisher information for the

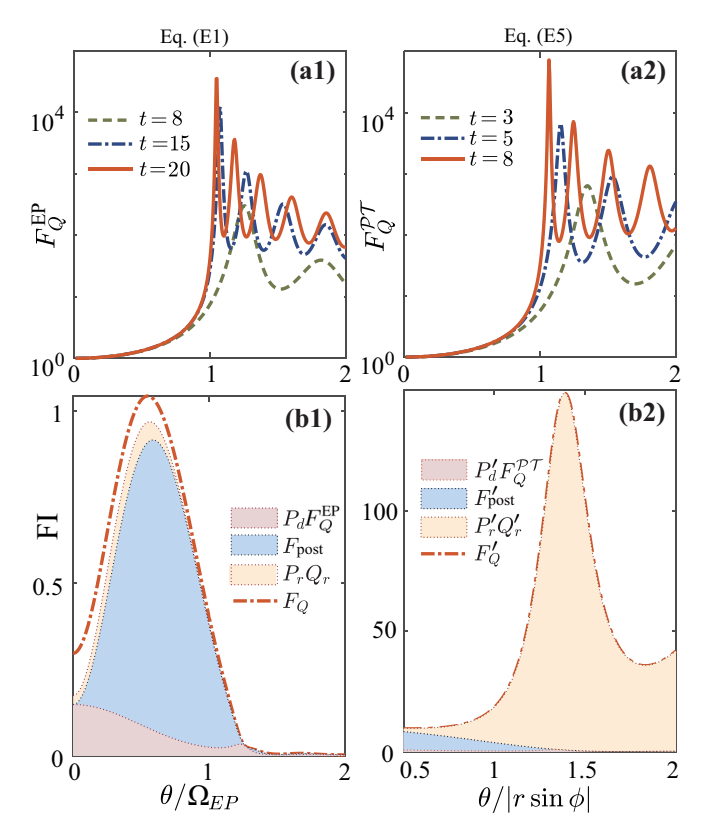


FIG. 4. Two exceptional-point-based sensors with Hamiltonians in Eqs. (E1) and (E5). (a1) The quantum Fisher information $F_Q^{\rm EP}$ for the sensor state (E1) for evolution times t=8,15,20, with $\Omega_{\rm EP}=\omega_{\rm ccw}$. (a2) QFI $F_Q^{\mathcal{PT}}$ for the sensor state (E5) for evolution times t=3,5,8, with $\phi=\pi/4$. (b1), (b2) The total effective QFI $F_{\rm post}$ and $F_{\rm post}'$, the effective QFI of EP-based sensors $P_dF_Q^{\rm EP}$ and $P_dF_Q^{\mathcal{PT}}$, the effective QFI for the rejected states P_rQ_r and $P_r'Q_r'$, and the Fisher information (FI) for postselection process $F_{\rm post}$ and $F_{\rm post}'$ are shown for t=8 and t=3, respectively.

rejected states $P'_rQ'_r$, and the Fisher information for postselection process itself F'_{post} , as shown in Fig. 4(b2). In addition, we also investigate the eigenvalues of $\hat{\eta}'(t)$ versus θ , as shown in Fig. 5.

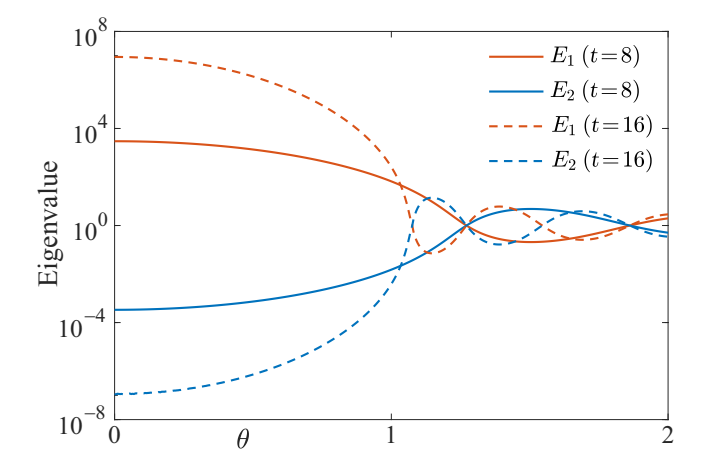


FIG. 5. Eigenvalues E_1 and E_2 of $\hat{\eta}'(t)$ for the model with a Hamiltonian in Eq. (E1), for t = 8, 16 and $\hat{\eta}'(0) = \mathbb{I}$.

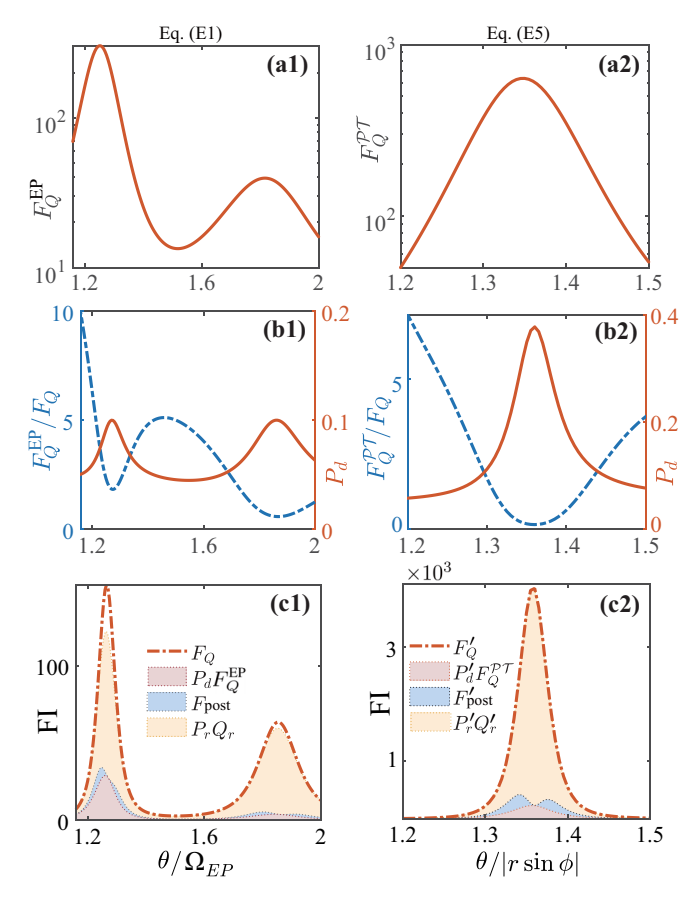


FIG. 6. Two exceptional-points-based sensors with Hamiltonians in Eqs. (E1) and (E5). (a1), (a2) QFI for two exceptional-points-based sensors for t=8 and 3, respectively. (b1), (b2) Ratios of the QFI for the exceptional-points-based sensors $F_Q^{\rm EP}$ and $F_Q^{\mathcal{PT}}$ to the total QFI F_Q and F_Q' for the dilated Hermitian systems (blue dashed-dotted curves) are compared with the success probabilities P_d and P_d' , respectively. (c1), (c2) The total QFI F_Q and F_Q' , the effective QFI for exceptional-points-based sensor states $P_dF_Q^{\rm EP}$ and $P_dF_Q^{\mathcal{PT}}$, the effective QFI for the rejected states P_rQ_r and $P_r'Q_r'$, and the FI for postselection process $F_{\rm post}$ and $F_{\rm post}'$ are shown for t=8 and t=3, respectively.

The exceptional point $(\theta=1)$ separates the phase diagram for a positive θ into two phases: the \mathcal{PT} -symmetry-broken phase $(0<\theta<1)$ and the \mathcal{PT} -symmetric phase $(\theta>1)$. In the \mathcal{PT} -symmetry-broken phase $(0<\theta<1)$, for any choice of $\hat{\eta}'(0)$, one eigenvalue of $\hat{\eta}'(t)$ will go infinity and the other approximates zero for $t\to\infty$. Therefore, a very large amplification factor $1/\nu'$ is required to multiply the $\hat{\eta}'(0)$ to ensure $[\hat{\eta}(t)-\mathbb{I}]$ as positive for a fixed evolution time, where ν' is the minimal eigenvalue of $\hat{\eta}'(t)$. Under this condition, the success probability P_d becomes extremely small; F_{post} and P_rQ_r account for the vast majority of F_{tot} . Since most of the measurement resources are discarded, the EP-based sensor in the \mathcal{PT} -symmetry-broken phase is very inefficient as: $F_Q\gg P_dF_Q^{\text{nH}}$. Here, we only consider the EP-based sensor in the \mathcal{PT} -symmetric phase.

Moreover, we use the time-independent dilation method to extend these two non-Hermitian systems, since this dilation method is simple, and the amplification factor $1/\nu_{\zeta}$ is much smaller than that in the time-dependent dilation method. The

results of both examples (as shown in Fig. 6) verify our theory $F_Q[|\Psi\rangle_{\rm SE}] \geqslant P_d F_Q^{\rm nH}[|\psi\rangle_{\rm S}]$, summarized as Eq. (4) in the main text

APPENDIX F: MODEL OF LOSS-LOSS \mathcal{PT} -SYMMETRY SENSOR

Finally, we consider a loss-loss \mathcal{PT} -symmetry sensor with a Hamiltonian as experimentally implemented in Ref. [25]:

$$H_{\rm LL} = \begin{pmatrix} v - ik_{\rm H} & ig\theta \\ -ig\theta & v - ik_{\rm V} \end{pmatrix},\tag{F1}$$

where θ is the unknown parameter to be estimated. Choosing $|\psi(0)\rangle$ as the initial state, the time-evolved state is

$$|\psi_{\rm LL}(t)\rangle = e^{-iH_{\rm LL}t} |\psi(0)\rangle$$
. (F2)

The Hamiltonian $H_{\rm LL}$ can be divided into two terms

$$H_{LL} = \begin{pmatrix} v - i\Delta k & ig\theta \\ -ig\theta & v + i\Delta k \end{pmatrix} - \begin{pmatrix} ik & 0 \\ 0 & ik \end{pmatrix}$$
$$= H_{GL} - ik\mathbb{I}, \tag{F3}$$

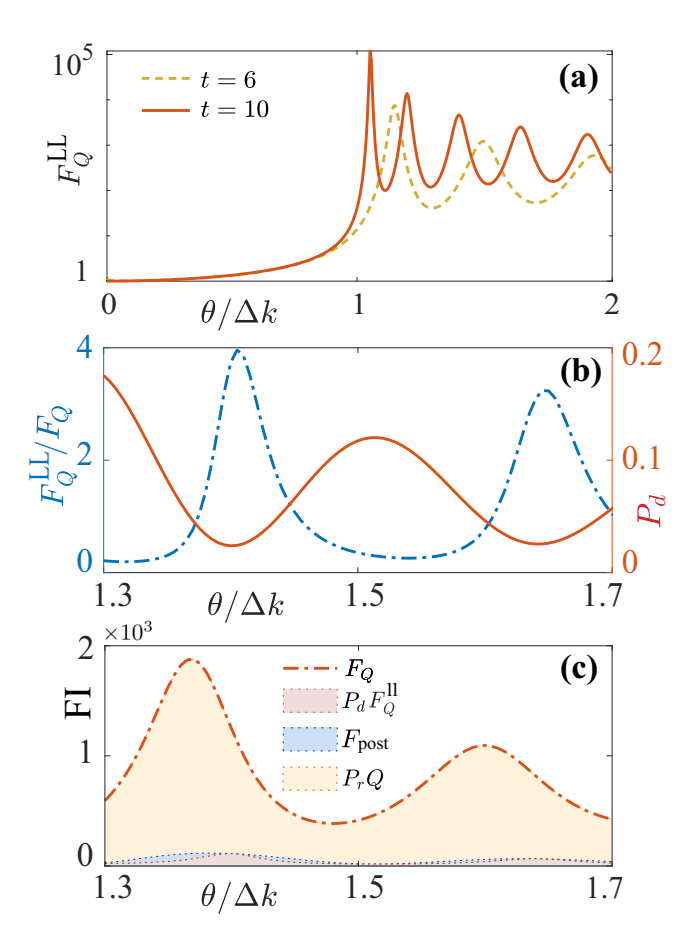


FIG. 7. Loss-loss \mathcal{PT} -symmetry sensor with a Hamiltonian (F1) and v=g=1. (a) QFI for the loss-loss sensor state for t=6 and 10. (b) Ratio of the QFI for the loss-loss sensor $F_Q^{\rm LL}$ to the total QFI F_Q for the Naimark dilated system (blue dashed-dotted curve) is compared with the success probabilities P_d (red solid curve). (c) Total QFI, F_Q , the effective QFI for the sensor state $P_dF_Q^{\rm LL}$, the effective QFI for the rejected state, and P_rQ_r , and the FI for postselection process, $F_{\rm post}$.

where $k = (k_{\rm V} - k_{\rm H})/2$, $\Delta k = (k_{\rm V} - k_{\rm H})/2$, and $H_{\rm GL}$ denotes the Hamiltonian of a gain-loss (GL) non-Hermitian system. After a gauge transformation, the evolution can be represented as

$$|\psi_{\rm LL}(t)\rangle_{\rm S} = e^{-iH_{\rm LL}t} |\psi(0)\rangle_{\rm S},$$
 (F4)

with $|\psi_{LL}(t)\rangle_S = \exp(-kt) |\psi_{GL}(t)\rangle_S$. That is, the dynamics of a loss-loss system is mathematically equivalent to that of a gain-loss system under the impact of a global exponential decay. Nevertheless, the loss-loss system can avoid the gain-induced noise.

Since the global exponential decay is independent of θ , we only focus on the $H_{\rm GL}$. The eigenenergies of $H_{\rm GL}$ are $E_{\pm} \equiv v \pm (\theta^2 - \Delta k^2)^{1/2}$, with the energy difference as $\Delta E = 2(\theta^2 - \Delta k^2)^{1/2}$, which vanishes as two exceptional points $(\theta = \pm \Delta k)$. By setting $|0\rangle_{\rm S}$ as the initial state, the time-evolved state under $H_{\rm GL}$ is

$$|\psi_{\rm GL}(t)\rangle_{\rm S} = [(a\cos at - \Delta k\sin at) |0\rangle_{\rm S} - \theta\sin at |1\rangle_{\rm S}]/C_{\rm GL},$$
(F5)

with $C_{\rm GL}=\theta^2-\Delta k^2\cos 2at-a\Delta k\sin 2at$, and $a=\Delta E/2$. The quantum Fisher information for the evolved state $F_Q^{\rm LL}[|\psi_{\rm LL}(t)\rangle_{\rm S}]$ can be arbitrary large for $t\to\infty$ near the exceptional points $(\theta/\Delta k=\pm 1)$, which is shown in Fig. 7(a).

Similarly, by extending the non-Hermitian system with the Naimark dilation method, we consider the ratio of the quantum Fisher information for the non-Hermitian sensors F_Q^{LL} to the one for the extended Hermitian system F_Q , which are compared with the postselection success probability P_d [see Fig. 7(b)]. In addition, we consider the effective quantum Fisher information of the non-Hermitian sensor, which is smaller than that one of its Hermitian counterpart as $P_d F_Q^{LL} < F_Q$ [Fig. 7(c)].

From Figs. 7(b) and 7(c), the effective quantum Fisher information of the non-Hermitian sensor $P_dF_Q^{\rm LL}$ achieves the maximum when the postselected probability P_d achieves its local minimum. It means more information of θ can be obtained with less trials of measurements using the non-Hermitian sensor from its Hermitian counterpart, i.e., "when less is more." However, the effective quantum Fisher information $P_dF_Q^{\rm LL}$ of the non-Hermitian sensor is still much smaller than that one for its Hermitian counterpart cause the loss of information during the postselection process. Our investigation employs quantum measurements with a weak probe, which inherently yields a low success probability. In contrast, classical measurements using a strong probe may achieve a higher success probability, presenting a problem for future research.

- [18] J. Wiersig, Enhancing the sensitivity of frequency and energy splitting detection by using exceptional points: Application to microcavity sensors for single-particle detection, Phys. Rev. Lett. 112, 203901 (2014).
- [19] C. Wang, C. Zhao, X. Li, E. Zhou, H. Miao, Y. Chen, and Y. Ma, Boosting the sensitivity of high-frequency gravitational wave detectors using PT-symmetry, Phys. Rev. D 106, 082002 (2022).
- [20] Z.-P. Liu, J. Zhang, Ş. K. Özdemir, B. Peng, H. Jing, X.-Y. Lü, C.-W. Li, L. Yang, F. Nori, and Y.-X. Liu, Metrology with PT-symmetric cavities: Enhanced sensitivity near the PT-phase transition, Phys. Rev. Lett. 117, 110802 (2016).

V. Giovannetti, S. Lloyd, and L. Maccone, Quantum metrology, Phys. Rev. Lett. 96, 010401 (2006).

^[2] V. Giovannetti, S. Lloyd, and L. Maccone, Advances in quantum metrology, Nat. Photon. 5, 222 (2011).

^[3] C. L. Degen, F. Reinhard, and P. Cappellaro, Quantum sensing, Rev. Mod. Phys. 89, 035002 (2017).

^[4] J. Kitching, S. Knappe, and E. A. Donley, Atomic sensors—a review, IEEE Sens. J. 11, 1749 (2011).

^[5] S. Aigner, L. D. Pietra, Y. Japha, O. Entin-Wohlman, T. David, R. Salem, R. Folman, and J. Schmiedmayer, Long-range order in electronic transport through disordered metal films, Science 319, 1226 (2008).

^[6] O. Hosten and P. Kwiat, Observation of the spin Hall effect of light via weak measurements, Science 319, 787 (2008).

^[7] L. Pezzè, M. Gabbrielli, L. Lepori, and A. Smerzi, Multipartite entanglement in topological quantum phases, Phys. Rev. Lett. 119, 250401 (2017).

^[8] Y.-R. Zhang, Y. Zeng, H. Fan, J. Q. You, and F. Nori, Characterization of topological states via dual multipartite entanglement, Phys. Rev. Lett. 120, 250501 (2018).

^[9] M. Brenes, S. Pappalardi, J. Goold, and A. Silva, Multipartite entanglement structure in the eigenstate thermalization hypothesis, Phys. Rev. Lett. 124, 040605 (2020).

^[10] X. Zhao, Y. Yang, and G. Chiribella, Quantum metrology with indefinite causal order, Phys. Rev. Lett. 124, 190503 (2020).

^[11] J.-Y. Desaules, F. Pietracaprina, Z. Papić, J. Goold, and S. Pappalardi, Extensive multipartite entanglement from SU(2) quantum many-body scars, Phys. Rev. Lett. 129, 020601 (2022).

^[12] Z. Li, S. Colombo, C. Shu, G. Velez, S. Pilatowsky-Cameo, R. Schmied, S. Choi, M. Lukin, E. Pedrozo-Peñafiel, and

V. Vuletić, Improving metrology with quantum scrambling, Science **380**, 1381 (2023).

^[13] M. P. Hokmabadi, A. Schumer, D. N. Christodoulides, and M. Khajavikhan, Non-Hermitian ring laser gyroscopes with enhanced Sagnac sensitivity, Nature (London) 576, 70 (2019).

^[14] S. Yu, Y. Meng, J.-S. Tang, X.-Y. Xu, Y.-T. Wang, P. Yin, Z.-J. Ke, W. Liu, Z.-P. Li, Y.-Z. Yang, G. Chen, Y.-J. Han, C.-F. Li, and G.-C. Guo, Experimental investigation of quantum \mathcal{PT} -enhanced sensor, Phys. Rev. Lett. 125, 240506 (2020).

^[15] Y.-H. Lai, Y.-K. Lu, M.-G. Suh, Z. Yuan, and K. Vahala, Observation of the exceptional-point-enhanced Sagnac effect, Nature (London) 576, 65 (2019).

^[16] H. Hodaei, A. U. Hassan, S. Wittek, H. Garcia-Gracia, R. El-Ganainy, D. N. Christodoulides, and M. Khajavikhan, Enhanced sensitivity at higher-order exceptional points, Nature (London) 548, 187 (2017).

^[17] W. Chen, Ş. K. Özdemir, G. Zhao, J. Wiersig, and L. Yang, Exceptional points enhance sensing in an optical microcavity, Nature (London) **548**, 192 (2017).

- [21] M. I. Rosa, M. Mazzotti, and M. Ruzzene, Exceptional points and enhanced sensitivity in \mathcal{PT} -symmetric continuous elastic media, J. Mech. Phys. Solids **149**, 104325 (2021).
- [22] Y. Tang, C. Liang, X. Wen, W. Li, A.-N. Xu, and Y. C. Liu, \mathcal{PT} -symmetric feedback induced linewidth narrowing, Phys. Rev. Lett. **130**, 193602 (2023).
- [23] Z. Li, C. Li, Z. Xiong, G. Xu, Y. R. Wang, X. Tian, X. Yang, Z. Liu, Q. Zeng, R. Lin, Y. Li, J. K. W. Lee, J. S. Ho, and C. W. Qiu, Stochastic exceptional points for noise-assisted sensing, Phys. Rev. Lett. 130, 227201 (2023).
- [24] J. Xu, Y. Mao, Z. Li, Y. Zuo, J. Zhang, B. Yang, W. Xu, N. Liu, Z. J. Deng, W. Chen *et al.*, Single-cavity loss-enabled nanometrology, Nat. Nanotechnol. **19**, 1472 (2024).
- [25] Y.-P. Ruan, J.-S. Tang, Z. Li, H. Wu, W. Zhou, L. Xiao, J. Chen, S.-J. Ge, W. Hu, H. Zhang, C.-W. Qiu, W. Liu, H. Jing, Y.-Q. Lu, and K. Xia, Observation of loss-enhanced magneto-optical effect, Nat. Photon. 19, 109 (2025).
- [26] C. E. Rüter, K. G. Makris, R. El-Ganainy, D. N. Christodoulides, M. Segev, and D. Kip, Observation of parity–time symmetry in optics, Nat. Phys. 6, 192 (2010).
- [27] B. Peng, Ş. K. Özdemir, F. Lei, F. Monifi, M. Gianfreda, G. L. Long, S. Fan, F. Nori, C. M. Bender, and L. Yang, Parity–time-symmetric whispering-gallery microcavities, Nat. Phys. **10**, 394 (2014)
- [28] L. Chang, X. Jiang, S. Hua, C. Yang, J. Wen, L. Jiang, G. Li, G. Wang, and M. Xiao, Parity-time symmetry and variable optical isolation in active-passive-coupled microresonators, Nat. Photon. 8, 524 (2014).
- [29] Ş. K. Özdemir, S. Rotter, F. Nori, and L. Yang, Parity-time symmetry and exceptional points in photonics, Nat. Mater. 18, 783 (2019).
- [30] M. Zhang, W. Sweeney, C. W. Hsu, L. Yang, A. D. Stone, and L. Jiang, Quantum noise theory of exceptional point amplifying sensors, Phys. Rev. Lett. 123, 180501 (2019).
- [31] H. Wang, Y.-H. Lai, Z. Yuan, M.-G. Suh, and K. Vahala, Petermann-factor sensitivity limit near an exceptional point in a Brillouin ring laser gyroscope, Nat. Commun. 11, 1610 (2020).
- [32] R. Kononchuk, J. Cai, F. Ellis, R. Thevamaran, and T. Kottos, Exceptional-point-based accelerometers with enhanced signal-to-noise ratio, Nature (London) **607**, 697 (2022).
- [33] K. J. H. Peters and S. R. K. Rodriguez, Exceptional precision of a nonlinear optical sensor at a square-root singularity, Phys. Rev. Lett. **129**, 013901 (2022).
- [34] W. Langbein, No exceptional precision of exceptional-point sensors, Phys. Rev. A 98, 023805 (2018).
- [35] J. Wiersig, Prospects and fundamental limits in exceptional point-based sensing, Nat. Commun. 11, 2454 (2020).
- [36] H. Loughlin and V. Sudhir, Exceptional-point sensors offer no fundamental signal-to-noise ratio enhancement, Phys. Rev. Lett. 132, 243601 (2024).
- [37] X. Zheng and Y. D. Chong, Noise constraints for nonlinear exceptional point sensing, Phys. Rev. Lett. 134, 133801 (2025)
- [38] J. Naikoo, R. W. Chhajlany, and J. Kołodyński, Multiparameter estimation perspective on non-Hermitian singularity-enhanced sensing, Phys. Rev. Lett. 131, 220801 (2023).
- [39] Y. Chu, Y. Liu, H. Liu, and J. Cai, Quantum sensing with a single-qubit pseudo-Hermitian system, Phys. Rev. Lett. **124**, 020501 (2020).

- [40] L. Xiao, Y. Chu, Q. Lin, H. Lin, W. Yi, J. Cai, and P. Xue, Non-Hermitian sensing in the absence of exceptional points, Phys. Rev. Lett. **133**, 180801 (2024).
- [41] J. Wiersig, Review of exceptional point-based sensors, Photon. Res. 8, 1457 (2020).
- [42] H.-K. Lau and A. A. Clerk, Fundamental limits and non-reciprocal approaches in non-Hermitian quantum sensing, Nat. Commun. 9, 4320 (2018).
- [43] L. Bao, B. Qi, D. Dong, and F. Nori, Fundamental limits for reciprocal and nonreciprocal non-Hermitian quantum sensing, Phys. Rev. A 103, 042418 (2021).
- [44] W. Ding, X. Wang, and S. Chen, Fundamental sensitivity limits for non-Hermitian quantum sensors, Phys. Rev. Lett. **131**, 160801 (2023).
- [45] C. M. Bender, Making sense of non-Hermitian Hamiltonians, Rep. Prog. Phys. 70, 947 (2007).
- [46] Y. Ashida, Z. Gong, and M. Ueda, Non-Hermitian physics, Adv. Phys. 69, 249 (2020).
- [47] C. M. Bender and D. W. Hook, PT-symmetric quantum mechanics, Rev. Mod. Phys. 96, 045002 (2024).
- [48] S. L. Braunstein and C. M. Caves, Statistical distance and the geometry of quantum states, Phys. Rev. Lett. **72**, 3439 (1994).
- [49] J. Ma, X. Wang, C. P. Sun, and F. Nori, Quantum spin squeezing, Phys. Rep. 509, 89 (2011).
- [50] B. M. Escher, L. Davidovich, N. Zagury, and R. L. de Matos Filho, Quantum metrological limits via a variational approach, Phys. Rev. Lett. 109, 190404 (2012).
- [51] B. Escher, R. L. de Matos Filho, and L. Davidovich, General framework for estimating the ultimate precision limit in noisy quantum-enhanced metrology, Nat. Phys. **7**, 406 (2011).
- [52] G. Tóth and I. Apellaniz, Quantum metrology from a quantum information science perspective, J. Phys. A: Math. Theor. 47, 424006 (2014).
- [53] Y. Aharonov, D. Z. Albert, and L. Vaidman, How the result of a measurement of a component of the spin of a spin-1/2 particle can turn out to be 100, Phys. Rev. Lett. 60, 1351 (1988).
- [54] A. G. Kofman, S. Ashhab, and F. Nori, Nonperturbative theory of weak pre- and post-selected measurements, Phys. Rep. **520**, 43 (2012).
- [55] J. Dressel, M. Malik, F. M. Miatto, A. N. Jordan, and R. W. Boyd, Colloquium: Understanding quantum weak values: Basics and applications, Rev. Mod. Phys. 86, 307 (2014).
- [56] S. Pang, J. Dressel, and T. A. Brun, Entanglement-assisted weak value amplification, Phys. Rev. Lett. 113, 030401 (2014).
- [57] J. Dressel, S. Agarwal, and A. N. Jordan, Contextual values of observables in quantum measurements, Phys. Rev. Lett. 104, 240401 (2010).
- [58] N. Dalla Pozza and M. G. A. Paris, Naimark extension for the single-photon canonical phase measurement, Phys. Rev. A 100, 032126 (2019).
- [59] R. Beneduci, Notes on Naimark's dilation theorem, J. Phys.: Conf. Ser. 1638, 012006 (2020).
- [60] M. Huang, R.-K. Lee, L. Zhang, S.-M. Fei, and J. Wu, Simulating broken \mathcal{PT} -symmetric Hamiltonian systems by weak measurement, Phys. Rev. Lett. **123**, 080404 (2019).
- [61] U. Günther and B. F. Samsonov, Naimark-dilated \mathcal{PT} -symmetric brachistochrone, Phys. Rev. Lett. **101**, 230404 (2008).

- [62] Y. Wu, W. Liu, J. Geng, X. Song, X. Ye, C.-K. Duan, X. Rong, and J. Du, Observation of parity-time symmetry breaking in a single-spin system, Science **364**, 878 (2019).
- [63] F. Minganti, A. Miranowicz, R. W. Chhajlany, I. I. Arkhipov, and F. Nori, Hybrid-Liouvillian formalism connecting exceptional points of non-Hermitian Hamiltonians and Liouvillians via postselection of quantum trajectories, Phys. Rev. A 101, 062112 (2020).
- [64] C. Ferrie and J. Combes, Weak value amplification is suboptimal for estimation and detection, Phys. Rev. Lett. 112, 040406 (2014).
- [65] G. C. Knee and E. M. Gauger, When amplification with weak values fails to suppress technical noise, Phys. Rev. X 4, 011032 (2014).
- [66] L. Zhang, A. Datta, and I. A. Walmsley, Precision metrology using weak measurements, Phys. Rev. Lett. 114, 210801 (2015).
- [67] J. Harris, R. W. Boyd, and J. S. Lundeen, Weak value amplification can outperform conventional measurement in the presence of detector saturation, Phys. Rev. Lett. 118, 070802 (2017).
- [68] N. Brunner and C. Simon, Measuring small longitudinal phase shifts: Weak measurements or standard interferometry? Phys. Rev. Lett. 105, 010405 (2010).
- [69] D. J. Starling, P. B. Dixon, A. N. Jordan, and J. C. Howell, Optimizing the signal-to-noise ratio of a beam-deflection measurement with interferometric weak values, Phys. Rev. A 80, 041803(R) (2009).
- [70] S. Pang and T. A. Brun, Improving the precision of weak measurements by postselection measurement, Phys. Rev. Lett. 115, 120401 (2015).
- [71] A. N. Jordan, J. Martínez-Rincón, and J. C. Howell, Technical advantages for weak-value amplification: When less is more, Phys. Rev. X 4, 011031 (2014).
- [72] G. C. Knee, J. Combes, C. Ferrie, and E. M. Gauger, Weak-value amplification: State of play, Quantum Meas. Quantum Metrol. 3, 32 (2016).
- [73] S. Tanaka and N. Yamamoto, Information amplification via postselection: A parameter-estimation perspective, Phys. Rev. A 88, 042116 (2013).
- [74] Y. Kim, S.-Y. Yoo, and Y.-H. Kim, Heisenberg-limited metrology via weak-value amplification without using entangled resources, Phys. Rev. Lett. **128**, 040503 (2022).
- [75] R. Jozsa, Complex weak values in quantum measurement, Phys. Rev. A 76, 044103 (2007).
- [76] Y.-T. Wang, J.-S. Tang, G. Hu, J. Wang, S. Yu, Z.-Q. Zhou, Z.-D. Cheng, J.-S. Xu, S.-Z. Fang, Q.-L. Wu *et al.*, Experimental demonstration of higher precision weak-value-based metrology using power recycling, Phys. Rev. Lett. 117, 230801 (2016).
- [77] L. Vaidman, Weak value controversy, Philos. Trans. R. Soc. Math. Phys. Eng. Sci. 375, 20160395 (2017).

- [78] Y. Aharonov, S. Massar, S. Popescu, J. Tollaksen, and L. Vaidman, Adiabatic measurements on metastable systems, Phys. Rev. Lett. 77, 983 (1996).
- [79] K. Lyons, J. Dressel, A. N. Jordan, J. C. Howell, and P. G. Kwiat, Power-recycled weak-value-based metrology, Phys. Rev. Lett. 114, 170801 (2015).
- [80] C. Helstrom, Quantum detection and estimation theory, J. Stat. Phys. 1, 231 (1969).
- [81] H. M. Wiseman and G. J. Milburn, Quantum Measurement and Control (Cambridge University Press, Cambridge, 2009).
- [82] J. Yang, Theory of compression channels for postselected quantum metrology, Phys. Rev. Lett. 132, 250802 (2024).
- [83] N. Okuma and M. Sato, Non-Hermitian topological phenomena: A review, Annu. Rev. Condens. Matter Phys. 14, 83 (2023).
- [84] I. Rotter, A non-Hermitian Hamilton operator and the physics of open quantum systems, J. Phys. A: Math. Theor. 42, 153001 (2009).
- [85] A. S. Holevo, Probabilistic and Statistical Aspects of Quantum Theory (North-Holland Publishing Company, Amsterdam, 1982).
- [86] A. S. Holevo, Statistical Structure of Quantum Theory, Lecture Notes in Physics Monographs (Springer-Verlag, Berlin, Heidelberg, 2001).
- [87] Y. Yu, L.-W. Yu, W. Zhang, H. Zhang, and X. Ouyang, Experimental unsupervised learning of non-Hermitian knotted phases with solid-state spins, npj Quantum Inf. 8, 116 (2022).
- [88] M.-A. Miri and A. Alù, Exceptional points in optics and photonics, Science 363, eaar7709 (2019).
- [89] R. El-Ganainy, K. G. Makris, M. Khajavikhan, Z. H. Musslimani, and S. Rotter, Non-Hermitian physics and PT symmetry, Nat. Phys. 14, 11 (2018).
- [90] M. Naghiloo, M. Abbasi, Y. N. Joglekar, and K. W. Murch, Quantum state tomography across the exceptional point in a single dissipative qubit, Nat. Phys. 15, 1232 (2019).
- [91] B. Peng, Ş. K. Özdemir, S. Rotter, H. Yilmaz, M. Liertzer, F. Monifi, C. M. Bender, F. Nori, and L. Yang, Loss-induced suppression and revival of lasing, Science 346, 328 (2014).
- [92] P. Wang, C. Chen, and R.-B. Liu, Classical-noise-free sensing based on quantum correlation measurement, Chinese Phys. Lett. **38**, 010301 (2021).
- [93] Y. Shen, P. Wang, C. T. Cheung, J. Wrachtrup, R.-B. Liu, and S. Yang, Detection of quantum signals free of classical noise via quantum correlation, Phys. Rev. Lett. 130, 070802 (2023).
- [94] N. Bobroff, Position measurement with a resolution and noise-limited instrument, Rev. Sci. Instrum. **57**, 1152 (1986).
- [95] M. Tsang, Ziv-Zakai error bounds for quantum parameter estimation, Phys. Rev. Lett. **108**, 230401 (2012).
- [96] N. Zeng, Codes for non-Hermitian sensing from the perspective of post-selected measurements.nb, figshare. Software. (2025), https://doi.org/10.6084/m9.figshare.29040953.v1.